.1

Part II
Microscopic Processes

Contents

.2

1 Thermal Equilibrium of the ISM

Thermal Equilibrium of the ISM

$$\underbrace{n\frac{d}{dt}\left(\frac{3}{2}kT\right)}_{\text{variation of internal E.}} \underbrace{-kT\frac{dn}{dt}}_{\text{power}} = \overbrace{\underbrace{\Gamma}_{\text{cooling rate}} - \underbrace{\Lambda}_{\text{heating}}}^{\text{J s}^{-1}\text{ cm}^{-3}}$$

In steady state, $dn/dt = dT/dt = 0$, so the temperature T is determined by $\Lambda(T) = \Gamma(T)$.

.3

1.1 Cooling of the ISM: detailed balance, critical density

Cooling of the ISM

Radiative cooling (ref. Dyson & Williams, Chap. 3, Spitzer, Chap. 4 & 6, Osterbrock, Chap. 3).

$$\begin{aligned} A+B &\rightarrow A+B^\star \\ B^\star &\rightarrow B+h\nu \end{aligned}$$

Requisites for a mechanism of radiative cooling

- frequent encounters, i.e. A & B abundant
- $E(B^\star)-E(B) \lesssim kT$.
- large rate of B excitations: high 'collision strength'
- time scale for radiative decay of $B^\star$ less than $\tau_{\rm col}$
- large escape probability of the output $h\nu$.

.4

Detailed balance: abundance of excited species

In steady state, the density n_j of species $B^\star$ in level j is determined by an equation of detailed balance, which models systems with a finite number of microscopic states:

$$\begin{aligned} &\sum_k \left(\left\{ \begin{array}{c} n_{\rm e} \\ n_{\rm H_2} \\ n_{\rm H_I} \end{array} \right\} n_j \gamma_{jk} + n_j B_{jk} J_\nu \right) + \sum_{k<j} \left(A_{jk} n_j \right) \\ &\quad = \sum_k \left(n_k \left\{ \begin{array}{c} n_{\rm e} \\ n_{\rm H_2} \\ n_{\rm H_I} \end{array} \right\} \gamma_{kj} + B_{kj} J_\nu n_k \right) + \sum_{k>j} \left(n_k A_{kj} \right), \end{aligned}$$

which we may also write using a simplified notation:

$$\sum_{i\neq j} n_j C_{ji} + n_j B_{ji} U_{\nu_{ji}} + \sum_{i<j} n_j A_{ji} = \sum_{i\neq j} n_i C_{ij} + n_i B_{ji} U_{\nu_{ij}} + \sum_{i>j} n_i A_{ij}.$$

.5

Detailed balance: rate of collisonal excitation

For any collision partner (i.e. either $\left\{ \begin{array}{c} n_{\rm e} \\ n_{\rm H_2} \\ n_{\rm H_I} \end{array} \right.$), the specific rate of collisional excitations is

$$\gamma_{jk} = \langle u \sigma_{jk}(u) \rangle = \frac{4}{\sqrt{\pi}} \left(\frac{m_r}{2kT} \right)^{3/2} \int_0^\infty du\, u^3 \sigma_{jk}(u) \exp\left(-\frac{m_r}{2kT} u^2 \right).$$

the specific rate (i.e. per pair of particles, in units of $\mathrm{m}^3\ \mathrm{s}^{-1}$) of collisional de-excitations γ_{kj} must be related to γ_{jk}: in thermodynamic equilibrium any microscopic process must be balanced by its inverse (*principle of detailed balance*, otherwise the distribution functions would depend on t and there would be no equilibrium).

.6

Milne relations

In **LTE** the rate of collisional excitations $j \to k$ with relative velocity $\vec{u} \in [\vec{u}, \vec{u} + d\vec{u}]$ must equal the rate of de-excitations $k \to j$ in the corresponding velocity range $\vec{v}$,

$$n_j^{\rm LTE} \begin{matrix} n_{\rm e} \\ n_{\rm H_2} \\ n_{\rm H_I} \end{matrix} \sigma_{jk}(u) f(u) u d\vec{u} = n_k^{\rm LTE} \begin{matrix} n_{\rm e} \\ n_{\rm H_2} \\ n_{\rm H_I} \end{matrix} \sigma_{kj}(v) f(v) v d\vec{v},$$

with $f(u) = \left(\frac{1}{\pi}\frac{m}{2kT}\right)^{3/2} \exp\left(-\frac{m}{2kT}u^2\right)$, and $\frac{1}{2}m_r v^2 = \frac{1}{2}m_r u^2 - E_{jk}$ [1],

$$\overset{\text{tarea}}{\Longrightarrow} \quad g_j u^2 \sigma_{jk}(u) = g_k v^2 \sigma_{kj}(v), \text{ or}$$

$$C_{kj} = C_{jk} \frac{g_j}{g_k} e^{E_{jk}/kT}.$$

.7

Critical density

The *critical density* is defined as the density at which the rate of collisonal de-excitations is equal to the rate of radiative de-excitations:

$$\sum_{k<j} C_{kj} = \sum_{k<j} A_{jk}.$$

A good cooling mechanism is therefore one that involves abundant species, an effective collision strength $\overset{>}{\sim}1$, a critical density $n_{\rm crit} \gg n_{\rm e}$, and opticallly thin transport of the output $h\nu_{jk}$.

.8

1.2 Ionic & atomic cooling of the ISM

Ionic & atomic cooling of the ISM

For ionic collisions, the cross-section of collisional excitation highlights the Coulomb cross-section.

$$\sigma_{jk}(E) = \frac{\pi a_\circ^2 \Omega_{jk}(E)}{E/E_\circ},$$

where $E_\circ$ is 1 Rydberg, $a_\circ$ is the Bohr radius, and $\Omega_{jk}(E)$ (of order 1), is the *collision strength* as a function of kinetic energy E. Finally the rate of excitations $j \to k$ (with units of $\rm s^{-1}$) is (tarea),

$$C_{jk} = \left\{ \begin{matrix} n_{\rm e} \\ n_{\rm H_2} \\ n_{\rm H_I} \end{matrix} \right\} \sqrt{\frac{2\pi}{kT}} \left(\frac{h}{2\pi}\right)^2 \frac{1}{m_r^{3/2}} \frac{\Gamma_{jk}}{g_j} e^{-E_{jk}/kT},$$

where Γ_{jk}, the *effective collision strength*, is the Maxwellian average of $\Omega(E)$.

.9

[1] note threshold excitation energy

Fine structure cooling in the IR

In LS coupling energy levels are ordered according to the Hund rules (Shu I Chap. 27):

- Higher S $\rightarrow$ lower energy
- Higher L $\rightarrow$ lower energy
- Higher J $\rightarrow$ higher energy if less than half-filled, lower energy if more than half-filled

Spectroscopic notation in spin-orbit coupling (ver Shu I,27): $^{2S+1}L_J$, with degeneracy (2 J+1)

Examples:

- [Ar VI] 4.52μm, $^2P_{\frac{1}{2}} \leftarrow ^2P_{\frac{3}{2}}$, Z=18
- [Al VI] 3.65μm, $^3P_2 \leftarrow ^3P_1$, Z=13

.10

Ar VI $^2P_{\frac{3}{2}}$ population

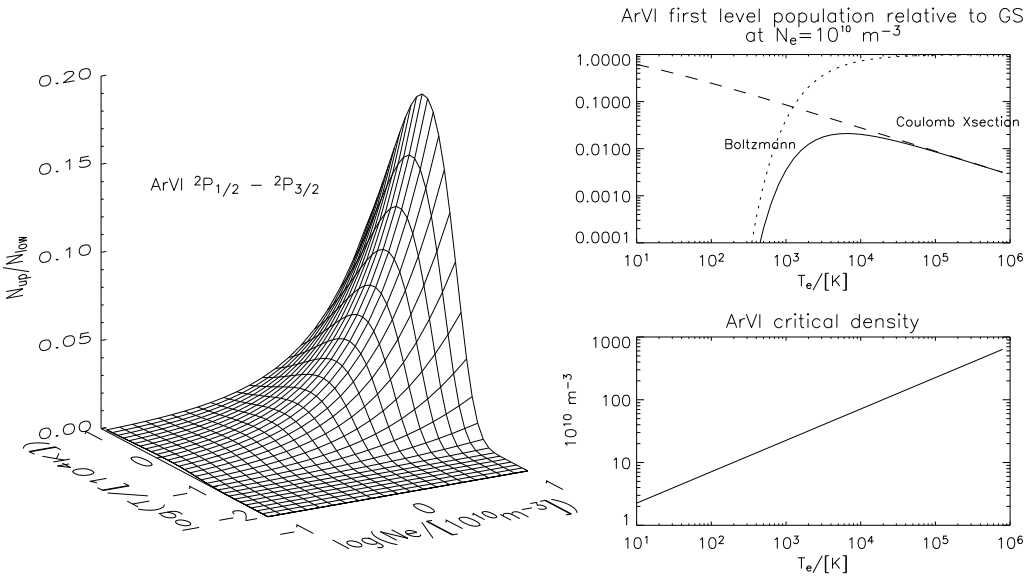

.11

Ar VI $^2P_{\frac{3}{2}}$ population

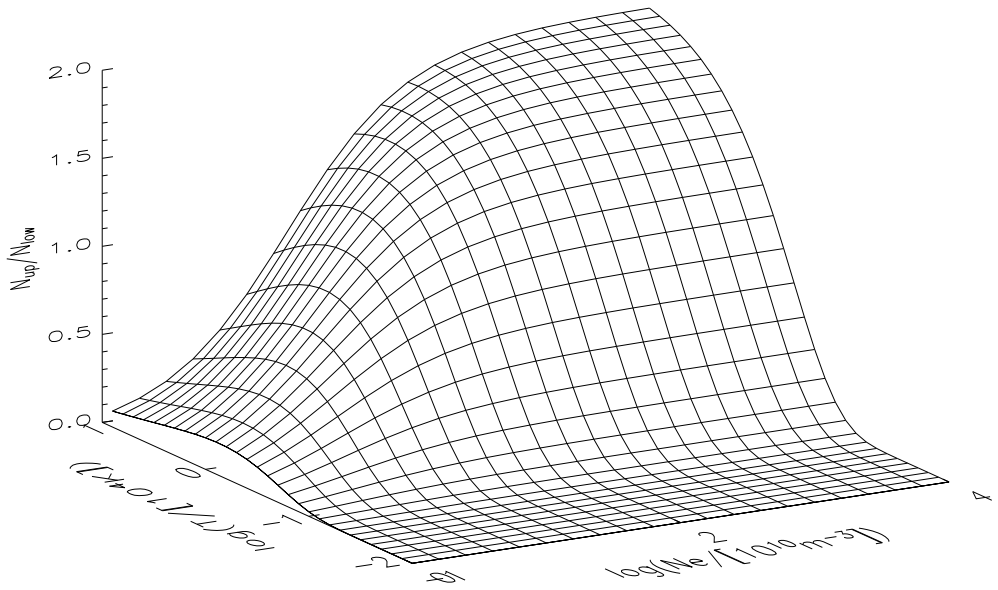

.12

Cooling of H II regions

- Collisional excitation of emission lines (case of a nebula photoionised by OB stars):
  - [O II]$\lambda\lambda$3726,3729 $^4\mathrm{S}_{3/2} \leftarrow^2 \mathrm{D}_{3/2,5/2}$.
  - [O III]$\lambda\lambda$4959,5007 $^3\mathrm{P}_{2,1} \leftarrow^1 \mathrm{D}_2$.
- continuum (free-free, bound-free): $A + B \rightarrow A + B + h\nu$ (postponed to chapter on photoionised nebulae)
- recombination (postponed to chapter on photoionised nebulae)

.13

Cooling of the neutral ISM

examples: Table 3.1 in Dyson & Williams complemented by the list of lines in `http://www.pa.uky.edu/~peter/atomic/`

Transition		collision partner	$\Delta E/k$
[C I] $\lambda 157.7\,\mu$m	$^2\mathrm{P}_{1/2} \leftarrow^2 \mathrm{P}_{3/2}$	H,e,H_2	92 K
[Si II] $\lambda 34.8\,\mu$m	$^2\mathrm{P}_{1/2} \leftarrow^2 \mathrm{P}_{3/2}$	e	92 K
[O I] $\lambda 63.2\,\mu$m	$^3\mathrm{P}_1 \leftarrow^3 \mathrm{P}_2$	H,e	228 K
[O I] $\lambda 145.5\,\mu$m	$^3\mathrm{P}_0 \leftarrow^3 \mathrm{P}_2$	H,e	326 K

.14

1.3 Molecular excitation & molecular structure

Molecular excitation - CO & H_2

ISO observations (Van Dishoeck, 2004, ARA&A, 42, 119) confirm that the contribution from H_2 cooling is more important than estimates based on *IRAS* data: H_2

is among the brightest emission lines in molecular clouds exposed to UV radiation, as for instance in Orion KL (note prominent dust continuuum):

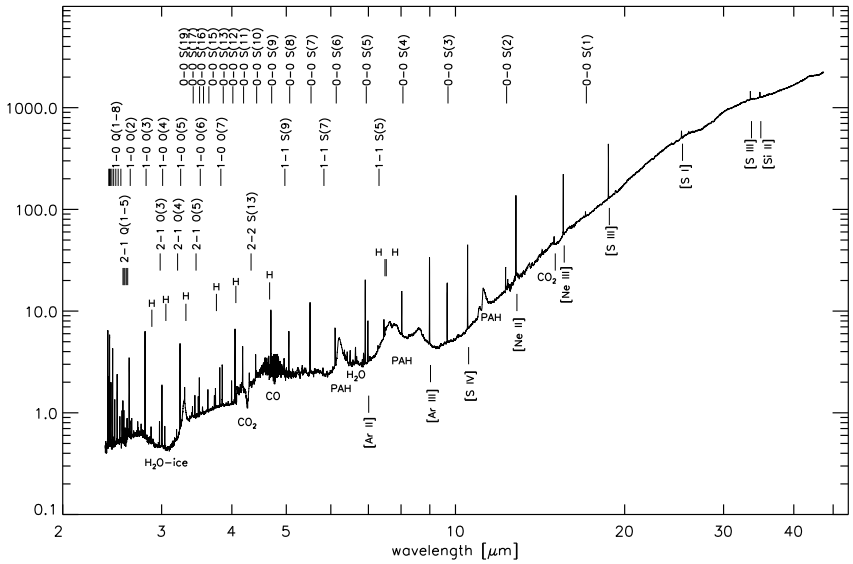

.15

fluorescent H_2: not a gas coolant

The rotational excitation of the ground vibrational state of H_2 is usually collisional (i.e. thermal), while higher vibrational states are excited by fluorescence (hence not a cooling process).

$\Rightarrow$ near-IR rovib H_2 is usually fluorescent, so not a coolant (except some of the lower-level rovib lines, in shocked regions).

.16

Dust continuum: not a gas coolant

The most luminous spectral component in the molecular ISM is the mid-IR to far-IR continuum, due to dust. Dust is responsible for transporting the UV radiation of the exciting stars, but is not always coupled to the molecular gas. Collisions are efficient dust heating sources in SNRs only.

.17

CO rotational-line cooling

The main cooling agents for cold molecular clouds are low-level rotational transitions of CO in the sub-mm. (Figure 2.11 from Tielens 2005).

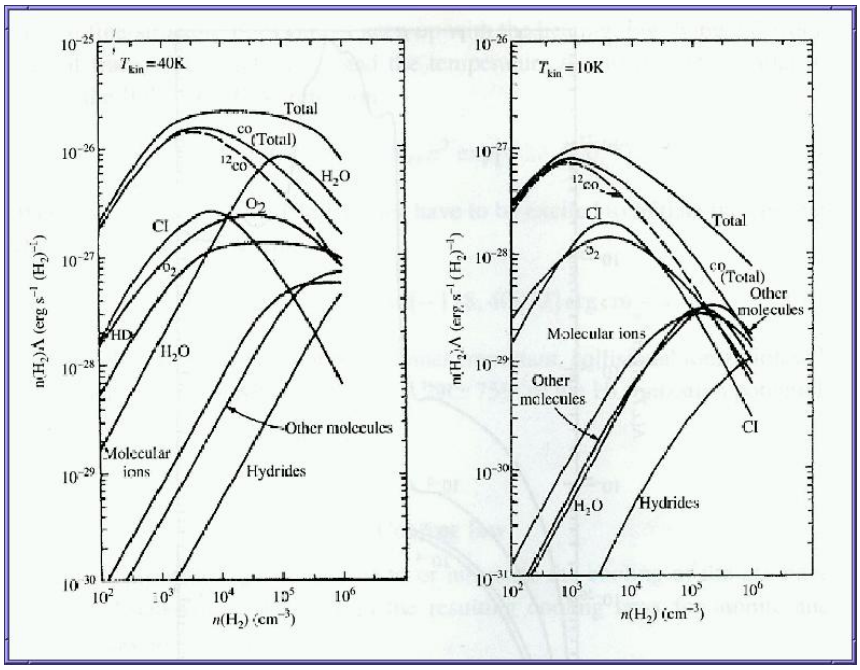

.18

Summary: diatomic molecules

In the Born-Oppenheimer approximation the Hamiltonian for a diatomic molecule AB separates, $H = H_{\rm AB} + H_{\rm el}$, where $H_{\rm AB}$ represents the kinetic energy of the nuclei, and $H_{\rm el}$ all the rest. It is also customary to factorize $\phi = \phi_{\rm el}\phi_{\rm AB}$ and obtain [2]:

$$H_{\rm el}\phi_{\rm el} = E_{\rm el}(R)\ \phi_{\rm el},$$

$$H_{\rm AB}\phi_{\rm AB} + E_{\rm el}(R)\ \phi_{\rm AB} = E\ \phi_{\rm AB},$$

and using the centre of mass coordinates, $\phi_{\rm AB} = \phi_{\rm trans}(\vec{X}_{\rm CM})\phi_{\rm intern}(\vec{R})$,

$$-\frac{\hbar^2}{2M}\nabla^2_{\rm CM}\phi_{\rm trans} = E_{\rm trans}\ \phi_{\rm trans}$$

$$-\frac{\hbar^2}{2\mu}\nabla^2_{\vec{R}}\phi_{\rm intern} + E_{\rm el}(R)\ \phi_{\rm intern} = E_{\rm intern}\ \phi_{\rm intern},$$

with $E = E_{\rm intern} + E_{\rm trans}$.

.19

[2] provided additional approximations according to Messiah, Vol. 2, XVIII.64 (p791), but exactly according to Shu I, 28. Probably valid only for processes slower than a rotation period.

The Laplacian in spherical coordinates,

$$\nabla^2_{\vec{R}} = \frac{1}{R^2}\left[\frac{\partial}{\partial R}\left(R^2\frac{\partial}{\partial R}\right) - \frac{L^2}{\hbar^2}\right],$$

inspires the decomposition of the wave function for the internal degrees of freedom in spherical armonics,

$$\phi_{\text{intern}}(\vec{R}) = \frac{1}{R}Z_{\text{vib}}(R)Y_{Jm}(\theta,\varphi),$$

The 1-D equation for $Z_{\text{vib}}(R)$ is a function of $E_{\text{el}}(R)$, the energy eigenvalue of the electronic wave function:

$$-\frac{\hbar^2}{2\mu}\frac{d^2Z_{\text{vib}}}{dR^2} + E_{\text{el}}(R)Z_{\text{vib}} = \left[E_{\text{intern}} - \frac{J(J+1)\hbar^2}{2\mu R^2}\right]Z_{\text{vib}}.$$

.20

In the armonic approximation we expand the 1-D equation for Z_{vib} about $R_\circ$, the AB separation in the fundamental state, highlighting the natural frequency $\mu\omega_\circ \equiv E''_{el}(R_\circ)$:

$$-\frac{\hbar^2}{2\mu}\frac{d^2Z_{\text{vib}}}{dx^2} + \frac{\mu}{2}\omega_\circ^2 x^2 Z_{\text{vib}} = E_{\text{vib}}Z_{\text{vib}},$$

$$x \equiv R - R_\circ, \quad \text{and}$$

$$\boxed{E_{\text{intern}} = E_{\text{el}}(R_\circ) + E_{\text{vib}} + E_{\text{rot}},}$$

$$E_{\text{rot}} = J(J+1)\frac{\hbar}{2\mu R_\circ^2} \equiv J(J+1)B, \quad B: \text{ rotational constant},$$

$$E_{\text{vib}} = (v+\frac{1}{2})\hbar\omega_\circ.$$

.21

The quantum numbers that determine the nuclear state of the molecule are J, m, v. Note the rigid body assumption: ϕ_{el} is independent of J, which is the fundamental hypothesis implicit in the decomposition $\phi = \phi_{\text{el}}\phi_{\text{AB}}$. The quantum numbers that characterise the electronic state of the molecule are Λ, and S, where Λ corresponds to the projection of L_{tot} along the internuclear axis[3], and S is the total spin.

.22

[3] the only component of $\vec{L}$ that is conserved in diatomic molecules

1.4 Atomic/molecular coupling with radiation

Interaction with electromagnetic radiation

The coupling term between charged particles and the electromagnetic field, $\vec{p}_i \cdot \vec{A}(\vec{k}\cdot\vec{x} - wt)$[4], can be expressed through an expansion in $\vec{k}\cdot\vec{x}$ as $H_{\rm int} = H_{\rm d} + H_{\rm M} + H_{\rm Q}$ (see Shu I,24), for which

$$H_{\rm d} = -\vec{E}\cdot\vec{d} \text{ (zeroth order)}$$

where, for a molecule, $\vec{d} = \vec{d}_{\rm el} + \vec{d}_{\rm nuc}$.

$$H_{\rm M} = -\vec{B}\cdot\vec{M} \text{ (first order)}$$

where the magnetic dipole moment $\vec{M} \propto \vec{L}$, and

$$H_{\rm Q} = -\frac{e}{6}\vec{\nabla}\vec{E} : (3\vec{x}\vec{x} - |\vec{x}|^2\mathbb{I}) \text{ (also order one).}$$

In general $H_{\rm M} > H_{\rm Q}$. .23

Bound-bound transition probabilities and cross-sections

In time-dependent perturbation theory, the rate of radiative excitations $i \to f$ is:

$$\frac{dP_{if}}{dt} \propto \mathfrak{N}(\omega_{if}) \left|\langle\phi_f|H_{\rm int}(\omega)|\phi_i\rangle\right|^2.$$

In a cubic box where the ocupation number of state $\vec{n}$ is $\mathfrak{N}$, the density of states is $d^3\vec{n} = V d^3\omega/(2\pi c)^3$, with a volume $V \to \infty$.

The absorption cross-section σ_{if} derives from $P_{if} = N_f/N_i \propto$ # of absorbed photons [5]:

$$P_{if} = \int d^3\vec{n}\,\frac{\mathfrak{N}(\vec{n})}{V} c\,t\,\sigma_{if} \;\Rightarrow\; \frac{dP_{if}}{dt} = \int_0^\infty \sigma_{if}\, c\, \mathfrak{N}(\omega)\,\frac{4\pi\omega^2}{(2\pi)^3 c^2} d\omega$$

Identifying (see Shu I, 22, 23), we obtain

$$\sigma_{if} \propto \left|\langle\phi_f|H_{\rm int}(w)|\phi_i\rangle\right|^2 \delta(\omega - \omega_{if}).$$

.24

Oscilator strength

For the electric dipole Hamiltonian, one gets

$$\sigma_{if} = \frac{4\pi^2}{3\hbar c}\left|\langle\phi_f|\vec{d}|\phi_i\rangle\right|^2 \delta(\omega - \omega_{if}),$$

which is usually expressed in terms of the oscilator strength f_{if},

$$\sigma_{if} = \frac{\pi e^2}{m_e c} f_{if}\,\delta(\nu - \nu_{if}), \;\; \text{con} \;\; f_{if} \equiv \frac{4\pi m_e}{3e^2\hbar}\nu_{if}\left|\langle\phi_f|\vec{d}|\phi_i\rangle\right|^2.$$

[4] when substituting $\vec{p} \to \vec{p} - \frac{q}{c}\vec{A}$, and neglecting terms in A^2 (OK for the ISM) see Shu I, 21

[5] note *optically thin* case: $dN_f = -\Gamma N_f dt + \frac{dP_{if}}{dt} N_i dt$.

For a single electron with position $\vec{x}$,

$$f_{if} = \frac{2m_e(\omega_{if}\langle f|\vec{x}|i\rangle)^2}{3\hbar w_{if}},$$

which is roughly the ratio between the vibrational potential energy of the electron and that of the radiated photon. .25

Relationship with Einstein coeficients

The equation of detailed balance,

$$n_i B_{if} J_{\nu_{if}} = n_f A_{fi} + n_f B_{fi} J_{\nu_{fi}},$$

and the LTE relationships,

$$\frac{n_f}{n_i} = \frac{g_f}{g_i}\exp(-\frac{h\nu_{if}}{kT}), \quad \text{and} \quad J_\nu = B_\nu(T), \quad \text{lead to}$$

$$A_{fi} = \frac{g_i}{g_f}(2h\nu^3/c^2)B_{if}, \qquad B_{fi} = \frac{c^2}{2h\nu^3}A_{fi} = (g_i/g_f)B_{if},$$

where the rate of stimulated excitations is related to the oscilator strength[6] :

$$B_{if} = \frac{4\pi^2}{h\nu}\frac{e^2}{m_e c}f_{if}.$$

.26

Selection rules

- Electric dipole
  - atoms: $\Delta l = 1$, $\Delta m = 0$.
  - molecules:
    - vibrational-rotational transitions, or rovibrational, $\Delta J = \pm 1$, $\Delta m = 0$,$\Delta v = \pm 1$, allowed when $\Lambda \neq 0$, $\Delta J = 0$ [7].
    - electronic transitions, $\Delta\Lambda = 0, \pm 1$, $\Delta S = 0$
    - electronic-vibrational-rotational transitions (i.e. *vibronic* transitions): $\Delta J = 0, \pm 1$, $\Delta m = 0, \pm 1$ and $\Delta J \neq 0$ si $\Lambda = \Delta\Lambda = 0$ and if $J = 0$.

      $$\Delta J = \begin{cases} +1 \ \rightarrow \ \text{R branch} \\ 0 \ \rightarrow \ \text{Q branch} \\ -1 \ \rightarrow \ \text{P branch} \end{cases}$$
- magnetic dipole, atoms: $\Delta l = 0$, $\Delta m = 0, \pm 1$.
- electric quadrupole, atoms: $\Delta l = 0, \pm 2$, $\Delta m = 0, \pm 1, \pm 2$, rotational transitions in molecules $\Delta J = 0, \pm 1, \pm 2$.

.27

[6] using the requirement $n_i B_{if} J_{\nu_{if}} = \int d\nu \int d\Omega \sigma_{if} n_i \frac{J_\nu}{h\nu} = \int d\nu 4\pi\sigma_{if} n_i \frac{J_\nu}{h\nu}$

[7] *Lambda doubling*, two states $\pm\Lambda$ for each J. Example: hyperfine structure of the OH Λ doublet at $\sim$1.7 GHz.

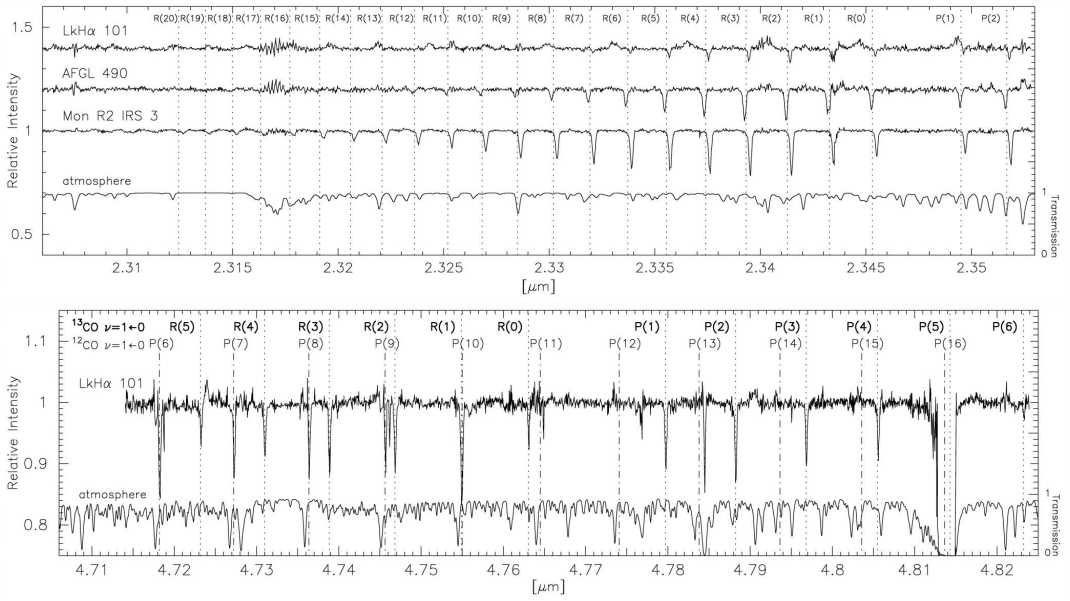

.28

Selection rules – H_2

In the case of H_2 we have $\vec{d} = 0$. Moreover the fundamental state is $\vec{L} = 0$, and $\vec{S} = 0$, so that $\vec{M} = 0$ and all low-energy transitions for H_2 are quadrupolar.

Note that the antisymmetry of the nuclear wave function implies that the state $J = 1$ (J odd) is triplet (**Ortho** H_2, $I = S_{\text{nuclear}} = 1$), while $J = 0$ (J even) is singlet (**Para** H_2, $I = 0$).

In H_2 the exclusion principle [9] forbids $\Delta J = 1$, unless the transition involves a change in spin state. The spin transitions can only occur through the exchange of protons in collisions. Radiative transitions between spin states can occur, but at a rate corresponding to the quadrupolar transitions in the Hamiltonian of the deviations to the Born-Oppenheimer approximations.

.29

In the ISM, **Ortho** and **Para** H_2 are effectively different molecules. The distinction extends to all molecules that contain H_2 radicals.

Rovibrational transitions between an upper level [1] and a lower level [2] are written $(v_1 - v_2)O(J_2)$, when $J_2 - J_1 = -2$, $(v_1 - v_2)Q(J_2)$ when $J_2 - J_1 = 0$, $(v_1 - v_2)S(J_2)$ when $J_2 - J_1 = +2$.

.30

[8] Subaru - IRCS + echelle & X-disperser, Goto et al. 2003, ApJ, 598, 1038

[9] the requirement that the wave function be antisymmetric

H_2 energy levels

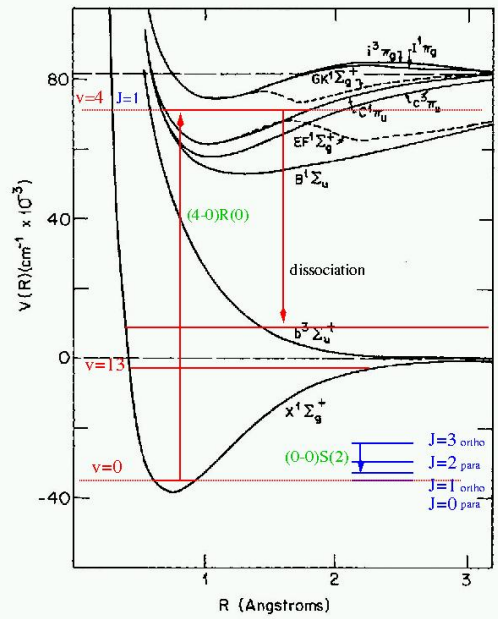

Figure 1 Total energy as a function of internuclear separation for low-lying states of H_2. Horizontal dashed lines denote total energy of two H atoms at infinite separation (both atoms in ground state; one atom in ground state and the other in the first excited states).

$\Lambda = 0, 1, 2, ...$
$\Leftrightarrow \Sigma, \Pi, \Delta$
levels in $E_{\rm el}(R)$:
X, B, C, D.

The energy separation between levels B and C with respect to X are $\sim$ 11 eV and 14 eV.

.31

Dissociation of H_2

The collisional dissociation of H_2,

$$\mathrm{H_2} + \begin{matrix}\mathrm{He}\\ \mathrm{H}\\ \mathrm{e}\end{matrix} \rightarrow 2\mathrm{H} + \begin{matrix}\mathrm{He}\\ \mathrm{H}\\ \mathrm{e}\end{matrix} ,$$

requires temperatures of order the binding energy of H_2, 4.48 eV$/k$ = 52000 K [10].

But an H_2 cloud is more likely to be photo-dissociated before it reaches 50 000 K. The dissociation continuum of H_2 (i.e. free states of H+H) starts 14.7 eV above the fundamental level of H_2 (i.e. $X^1\Sigma$, para-H_2), while the ionization continuum (the ejection of one electron) starts at 15.4 eV. Both continua, ionising and dissociating, lie above 13.6 eV. In the context of a molecular cloud surrounded by H I, the H_2 dissociating radiation is completely absorbed by the Lyman continuum of H I.

.32

Dissociation of H_2

The likeliest mechanism for H_2 dissociation is absorption to the robrivational bands of excited electronic states (e.g. B o C), and

1. subsequent de-excitation to dissociated levels of lower energy (e.g. $b^3\Sigma$), or
2. decay to the vibrational continuum of electronic state X (with $v \geq 14$), or
3. decay to excited levels of the fundamental state and subsequent absorption to the dissociating continuum (one order of magnitude slower than mechanisms 1) and 2) , Stecher& Williams 1967, ApJ 149, L29)

.33

IR emission from H_2

Since the rate of radiative transitions within the ground state electronic level of H_2 is quadrupolar, the distribution of ro-vibrational population is dominated by collisions between H_2 molecules.

If $kT \gg \Delta E_{\rm FIR}$, the typical energy difference between rotational levels of ground state H_2, the occupation numbers of the robrivational levels in the ground state electronic state follow LTE:

$$N(v,J) \propto \omega(J) \exp(-B\,(J\,(J+1))/kT),$$

in which $\omega(J) = 3 \times (2J+1)$ for ortho-H_2, and $\omega(J) = 1 \times (2J+1)$ for para-H_2. This situation (i.e. hot molecular gas) is typical of shocks in the ISM.

In the presence of an intense UV field the IR emission of H_2 is fluorescent (Black & Van Dishoeck, 1987, ApJ, 322, 412). Fluorescence dominates if $kT \ll \Delta E_{\rm FIR}$. The absorption of one UV photon excites H_2 to an electronic state, leading to photodissociation (with a 15% probability), and to an IR cascade in all other cases.

.34

IR emission from H_2

Example excitation diagram for the Helix nebula.

[10] the law of mass-action does not change this result because the number of continuum states accessible to both products and reactants is similar, in contrast with ionisation, which is described by the Saha equation

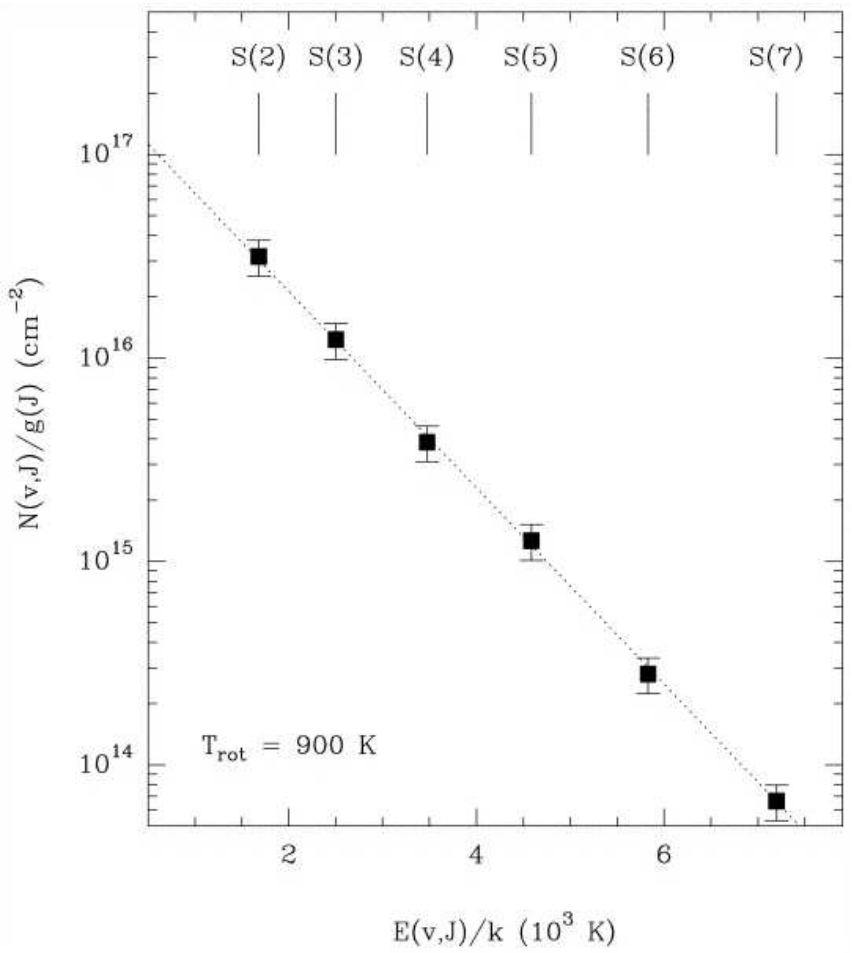

IR emission from H_2, ζ Oph

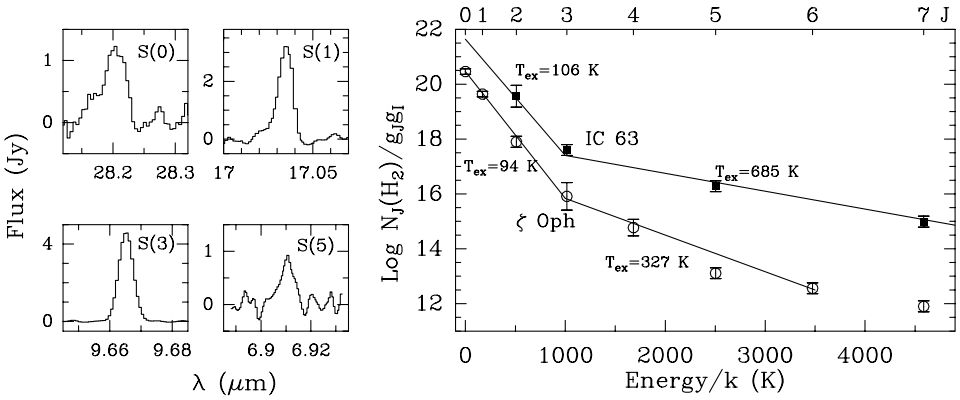

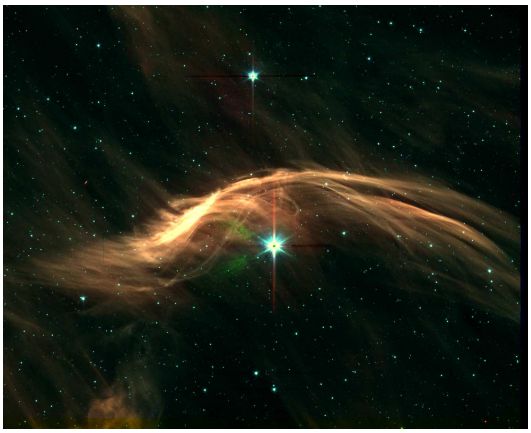

.36

1.5 Heating of the ISM

Heating of the neutral ISM

H_2 is an important source of UV opacity, as shown in the *FUSE* spectra of HD210839 and HD154368 (Rachford et al., 2002, ApJ, 577, 221).

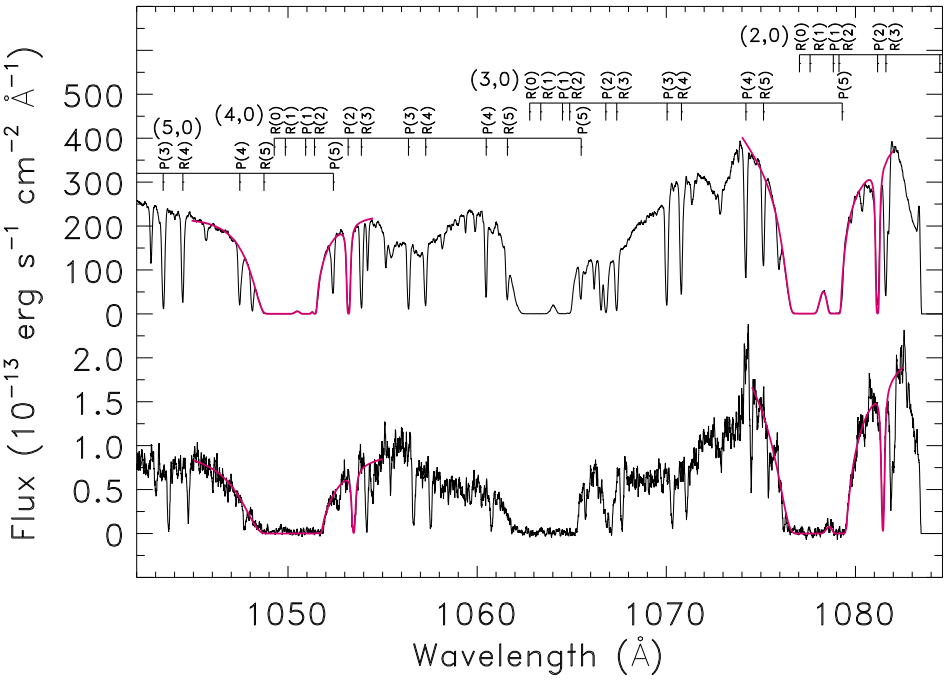

.37

- heating by photodissociation and photoionisation:

$$AB + h\nu \rightarrow A + B,$$

dominated by H_2 photodissociation.
- collisional de-excitation (in particular for H_2, when $n(H_2) > 10^4$ cm^{-3}).
- heating by photoionisation:

$$A + h\nu \rightarrow A^+ + e,$$

in the case of the neutral ISM, photoionisation heating is dominated by C^+, with an ionization potential of 11.3 eV. The average kinetic enery of the ejected electron is

$$\frac{3}{2}kT_i = \frac{\int_{\nu_i}^{\infty}(J(\nu)/h\nu)\alpha_i(\nu)h(\nu-\nu_i)d\nu}{\int_{\nu_i}^{\infty}(J(\nu)/h\nu)\alpha_i(\nu)d\nu}.$$

.38

- photoelectric effect on dust grains. The grain heating efficiency, $\varepsilon_{\rm grain}$, defined as the ratio between output gas heating and input UV radiation (Tielens Chap. 3.3.1), is

$$\varepsilon_{\rm grain} = Y \times \frac{h\nu - W - \phi}{h\nu},$$

where the electron escape probability Y is the ratio between the e^- - e^- mean free path $l_e \approx 10$ Å, and the absorption depth of UV radiation, $l_a \approx 100$ Å: $Y \approx l_e/l_a$. W is the work function of the grain and $\phi = Z \times e^2/a$ is the surface potential for a grain of size a. The ionization potential of a grain is thus $I = W + \phi$. The heating efficiency is larger for smaller grains, since $l_a \approx l_e$. The ejection of photoelectrons from grains is the dominant heating source in the neutral ISM exposed to FUV radiation, as in the case of PDRs. Photoionisation is dominant in the case of the ionised gas.

.39

- The total photoelectric heating rate from grains per unit volume, $n\Gamma_{\rm grain}$, can be written:

$$n\Gamma_{\rm grain} = \int_{a_{\rm min}}^{a_{\rm max}} n(a)da \sum_i \int_{\nu_i}^{\nu_{\rm H}} \frac{J_\nu}{h\nu}\alpha_{\rm grain,i}(\nu)E_{\rm kin}(a,i)d\nu,$$

where a is grain diameter, and i runs over grain ionisation stage, and $h\nu_{\rm H} = 13.6$ eV.
- in addition to photo-electric heating, grains can also heat the gas through inelastic collisions if the solid state temperature is larger than the gas temperature.

.40

- heating from cosmic rays: Important for molecular phase. Cosmic rays, as well as X-rays, ionise H_2 (IP=15.4 eV):

$$H_2 + (p, e^-, \alpha, X) \rightarrow H_2^+ + e^- + (p, e^-, \alpha, X)',$$

followed by the formation of H_3^+:

$$H_2^+ + H_2 \rightarrow H_3^+ + H.$$

An important mechanism for the destruction of H_3^+ is its dissociative recombination,

$$H_3^+ + e \rightarrow \begin{cases} 3H \\ H_2 + H \end{cases}$$

Since both the formation and the destructionof H_3^+ are exothermic (the energy released into the ISM in the process is 11 eV), the H_3^+ cycle is a heating source of the ISM.

.41

- Turbulent heating.
Important in molecular clouds at ~ 10 K, without UV field.
In a turbulent flow the kinetic energy density will trickle down a hierarchy of scales, until it is dissipated by diffusion at the smallest scale fixed by viscosity. The timescale for downwards energy transfer at scale l can be approximated with the crossing time at the velocity disperson v. Thus the rate of heating per unit volume is (Tielens 3.8),

$$n\Gamma_{\text{turbulence}} = \frac{1}{2}\frac{n\, m_H v^2}{l/v}.$$

The observations of the energy density and velocity dispersion at a given scale l leads to an estimate of turbulent heating.
The energy densities as a function of scale can be calculated assuming a constant energy transfer rate: $v^2/(l/v)$ is constant.

.42

2 Molecule formation

2.1 Grain catalysis

Molecule formation

The encounter of two atoms A and B, initially unbound, will lead to molecular synthesis if:

1. bound states of AB exist.

2. There is a mechanism for molecular stabilization faster than the lifetime of the $AB^\star$ state [11], of order $\sim 10^{-13}$ s ($\approx$ 1 vibrational period).

Radiative dissipation of the energy excess of $AB^\star$ is improbable: even for electric dipole decay rates, about 10^8 s^{-1} in the UV, only 1 out of 10^5 collisions will produce a molecule.

The abundance of H_2 might raise the low probability of condensation via collisions, but the electric dipole transitions of H_2 are fobbiden. H_2 cannot associate radiatively.

The H_2 half-life in the diffuse interstellar UV radiation field is of $\sim$ 300 yr $\Rightarrow$ some other mechanism must exist for efficient H_2 formation. .43

Grain catalysis of the formation process of H_2

The adsorption of hydrogen atoms onto the surface of dust grains allows raising the available timescale for the $A + B$ encounter, and the grain acts as stabilizing agent by absorbing the excess energy of $AB^\star$.

Once H_2 is formed, its 4.48 eV of binding energy (the first bound-free transition is at 2500 Å) eject H_2 from the grain surface, and the excess of energy over the grain work function is distributed over the molecular degrees of freedom, leaving the H_2 molecule in an excited state.

IR transitions from the formation pumping of excited levels of H_2 were observed by Burton et al. (2002, MNRAS, 333, 721) in M 17: the line (6-4)O(3) at 1.73μm cannot be collisionally excited since its superior level is at $\Delta E/k \sim$30 000 K above ground, yet the intensity of (6-4)O(3) relative to other H_2 lines does not match fluorescent models. .44

2.2 Ion-molecule chemistry

Molecule formation - the role of H_3^+

• H_3^+ controls the ionisation stage of the molecular ISM.

The H_3^+ cycle with corresponding rates is:

$$H_2 + (p, e^-, \alpha, X) \xrightarrow{\zeta} H_2^+ + e^- + (p, e^-, \alpha, X)',$$

$$H_2^+ + H_2 \xrightarrow{\eta_1} H_3^+ + H,$$

$$H_3^+ + e \xrightarrow{\eta_2} H_2 + H,$$

where ζ is the ionization rate of H_2, in s^{-1}. We see that

$$\zeta n_{H_2} = \eta_1 n_{H_2} n_{H_2^+}, \text{ and}$$

$$\eta_2 n_{H_3^+} n_e = 2\zeta n_{H_2}$$

With canonical values for the rates η_i, one gets $n_{H_3^+} \gg n_{H_2^+}$, and the requisite for neutrality $n_e \approx n_{H_3^+}$ allows concluding $n_e/n_{H_2} \approx 10^{-8}$ . .45

[11] the molecule is initially bound at a level with energy equal to that of the colliding pair

Ion-molecule chemistry

• In ion-molecule chemistry, the standard model for interstellar chemistry, H_3^+ is cornerstone to all reaction cycles:

The cycle of an element X (anything short of He, O_2,...) is initiated by H_3^+ through

$$H_3^+ + X \rightarrow XH^+ + H_2, \text{ and subsequently,}$$

$$XH^+ + Y \rightarrow XY^+ + H.$$

Example: production of H_2O and OH,

$$H_3^+ + O \rightarrow OH^+ + H_2, \text{ followed by the sequence,}$$

$$OH^+ + H_2 \rightarrow {OH_2}^+ + H,$$

$$OH_2^+ + H_2 \rightarrow {OH_3}^+ + H,$$

and finally one dissociative recombination

$${OH_3}^+ + e \rightarrow \begin{cases} H_2O + H \\ OH + H_2 \end{cases}.$$

.46

The full story

• Molecular formation: realistic cycles (Sternberg & Dalgarno 1995, ApJSS, 99, 565).

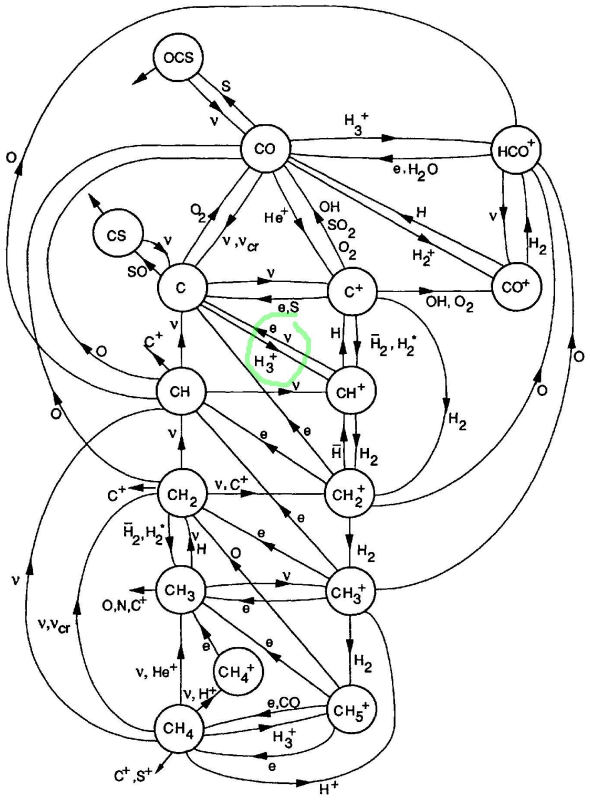

.47

2.3 Observational validation

Molecular formation - validation of the ion-molecule chemical model

.48

H_3^+, the pilar of chemical cycles in the ISM, was detected by Geballe & Oka (1996, *Nature*, 384, 334; Geballe 2000, *Phil.Trans.R.Soc.Lond.*A, 358, 2503), with an abundance close to that expected from the ionization fraction.

H_3^+ does not have electric dipole moments, and is even worse than H_2: it is deprived of excited electronic states (i.e. no UV transitions). It only has two vibration modes. One is symmetrical, ν_1, that does not induce electric dipole moment and does not radiate. Only the asymmetrical mode ν_2 induces an electric dipole.

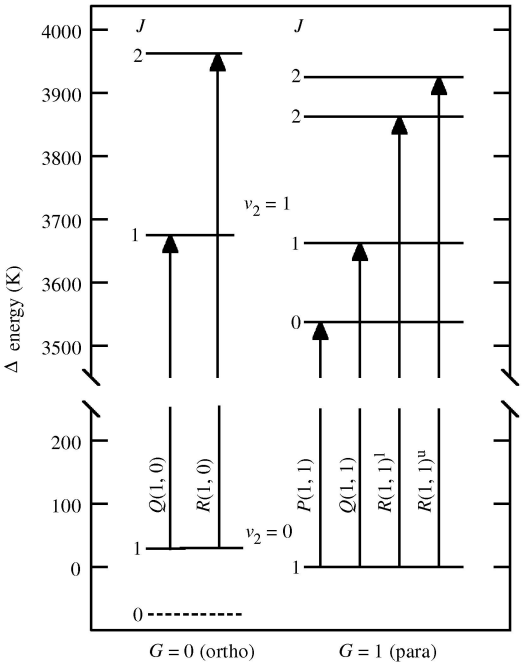

The production of H_3^+

$$H_2 + (p, e^-, \alpha, X) \xrightarrow{\zeta} H_2^+ + e^- + (p, e^-, \alpha, X)',$$

$$H_2^+ + H_2 \xrightarrow{\eta_2} H_3^+ + H,$$

is balanced by its destruction, mainly through

$$H_3^+ + CO \xrightarrow{\eta_{CO}} COH^+ + H_2,$$

equating rates, one gets

$$2\zeta n_{H_2} = \eta_{CO} n_{H_3^+} n_{CO},$$

in which $\eta_{CO} = 1.8\ 10^{-9}\ s^{-1}$, and $\zeta = n_{p,X,\alpha,e^-}\ \eta_1 \approx 3\ 10^{-17}\ s^{-1}$, gives the product of the cosmic ray density times the ionisation rate of H_2. In general the relative abundances of CO and H_2 are constant in the diffuse ISM (model: Lee et al., 1996, A&AS, 119, 111, observations: Federman et al. 1980, ApJ 242, 545), $n_{CO}/n_{H_2} = 1.5\ 10^{-4}$, so that

$$\boxed{n_{H_3^+} \approx 10^{-4}\ cm^{-3},\ \text{ independent of } n_{H_2}}$$

For typical densities $n_{H_2} \approx 10^4 cm^{-3}$, we have $N_{H_3^+} \approx 10^{-9} N_{H_2}$!!

.49

Detection of H_3^+, Oka & Geballe

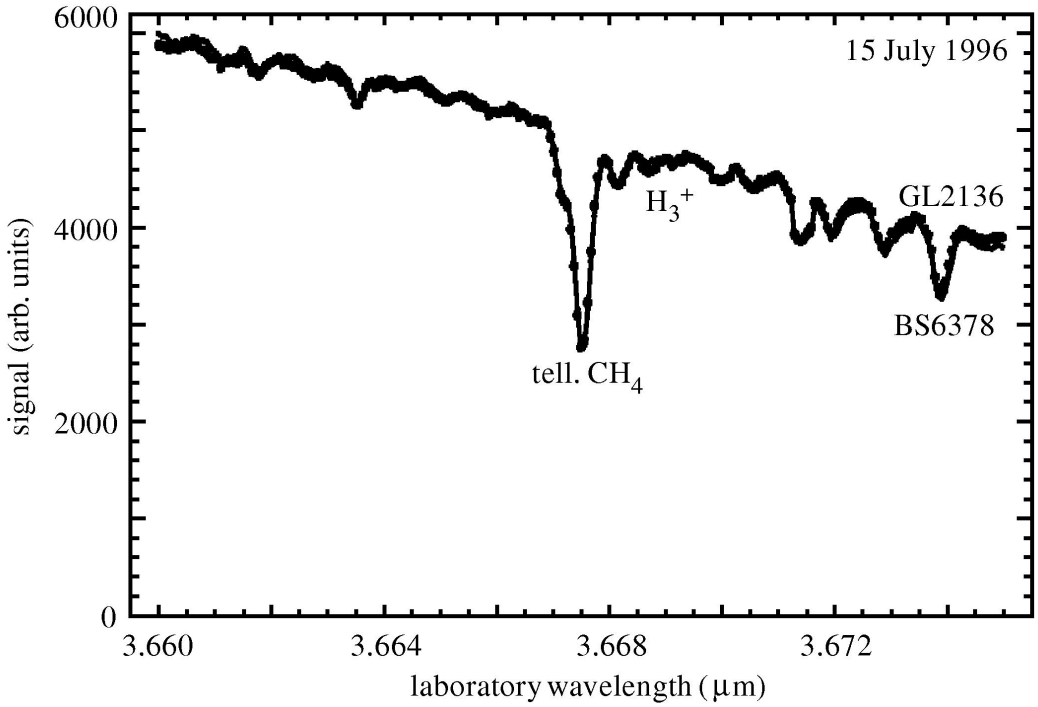

.50

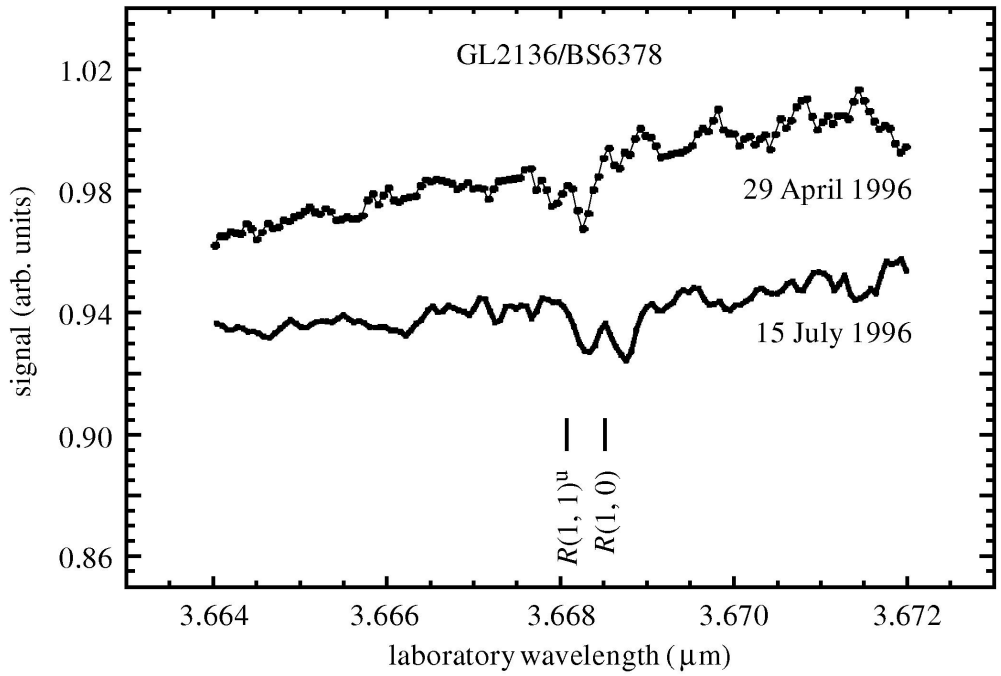

.51

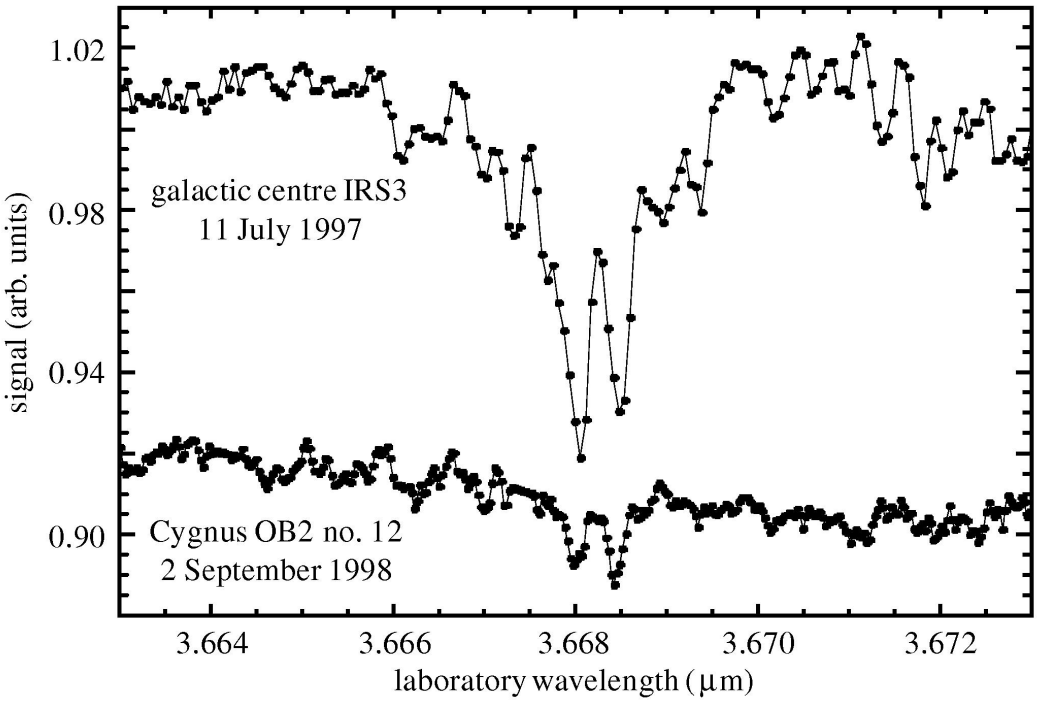

.52

3 Chemical fractionation

Chemical fractionation: CO

The reaction

$$^{13}\mathrm{C}^{+} + {}^{12}\mathrm{CO} \underset{k_2}{\overset{k_1}{\rightleftharpoons}} {}^{12}\mathrm{C}^{+} + {}^{13}\mathrm{CO} + \Delta E,$$

is slightly exothermic: $\Delta E/k = 35$ K. Consequently, at low temperatures ($\lesssim 35$ K), the isotopic ratio $^{12}\mathrm{C}/^{13}\mathrm{C}$ is different in CO than in the rest of the ISM - there is fractionation in the C isotopes.

.53

Chemical fractionation: theory

At constant P and T, minimizing the free energy G gives $\sum_i \nu_i \mu_i = 0$, and allows relating the concentration of each species involved in the reaction. For reactions in the gas phase, we can use the chemical potential of ideal gases, $\mu_i = kT \ln[n_i/\mathscr{Z}_i(T)]$, with the partition function

$$\mathscr{Z}_i(T) = \frac{h}{\sqrt{2\pi m_i\, kT}} \sum_a g_i^a e^{-\xi_a/kT},$$

where the energies associated with the internal degrees of freedom are referred to the ground state. We get the law of mass-action (e.g. Shu I, 7),

$$\prod_i n_i^{\nu_i} = \prod_i \mathscr{Z}_i^{\nu_i}.$$

.54

Application to CO

For CO fractionation,

$$\frac{n(^{13}C^{+})\, n(^{12}CO)}{n(^{12}C^{+})\, n(^{13}CO)} = e^{-\frac{1}{kT}\left(\xi(^{12}CO)-\xi(^{13}CO)\right)} = \exp\left(-\frac{\Delta E}{kT}\right),$$

where the ground state energy is $\xi(^{12}CO)$.

For CO, the rates of reactions in both directions are fast, $k_1 = k_2 = 2\ 10^{-10}$ cm^3 s^{-1}, and for cold clouds with $n(H_2) \approx 10^4$ cm^3 and $n_{CO}/n_{H_2} \approx 10^{-4}$, the relaxation time is $\tau_{frac} \lesssim 1000$ yr. Thus CO is enriched in ^{13}C, at the expense of the rest of the molecules.

The work function of a dust grain for the adsorption of CO is $\Delta H \sim$900 K, and for $T \lesssim 900$ K the probability of adsorption for grain-CO collisions is 1. Besides the vapor pressure of CO is very high compared to typical ISM pressures (Leger, 1983, A&A, 123, 271). CO is expected to be substantially (of order 50%) condensed onto icy CO mantles on the surface of grains (Whittet et al. 1985, MNRAS, 216, 45). .55

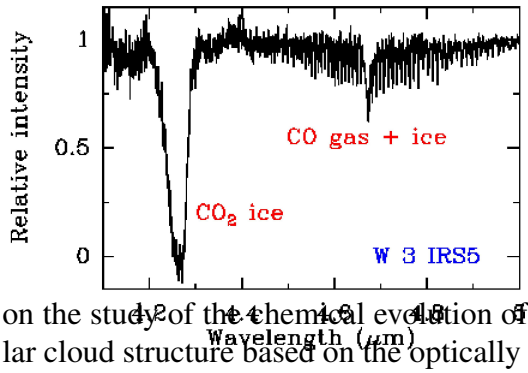

We see that the isotopic ratio ^{12}C/^{13}C will be different in the dust than in the gas phase. Additionally the C ratio in any given molecule of the gas phase will depend on the details of the synthesis reactions. The position taken by CO in relation to C^+ will determine the C ratio in the product molecule. This result bears on the study of the chemical evolution of galaxies, as well as on studies of molecular cloud structure based on the optically thin isotopes.

Chemical fractionation competes with the process of selective photodissociation. ^{13}CO is dissociated by interstellar UV radiation, penetrating to deeper lying layers in the clouds than for the main isotope, ^{12}CO. .56